Yuzuncu Yil University
Journal of the Institute of Natural & Applied Sciences

https://dergipark.org.tr/en/pub/yyufbed

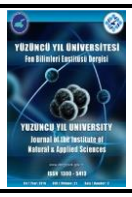

Research Article

Focusing on Some Physical Properties of Li_2TlIn: an Ab Initio Study

Nihat AYDIN[1], Emel KİLİT DOĞAN*[2]

[1] Van Yuzuncu Yil University, Institute of Natural and Applied Sciences, Physics Department 65080, Van, Turkey
[2] Van Yuzuncu Yil University, Faculty of Science, Physics Department 65080, Van, Turkey

Nihat AYDIN, ORCID No: 0000-0001-5580-6982, Emel KİLİT DOĞAN, ORCID No: 0000-0001-7609-7206
*Corresponding author e-mail: ekilit@yyu.edu.tr

Article Info

Received: 11.04.2022
Accepted: 25.06.2022
Online December 2022
DOI: 10.53433/yyufbed.1101619

Keywords
Dynamic properties,
Elastic properties,
Electronic properties,
Heusler compound,
Li_2TlIn

Abstract: Structural, electronic, elastic and dynamic properties of Li_2TlIn were studied for the ground state (i. e. P = 0 kbar) and under pressure value of 4.53 kbar, using Density Functional Theory (DFT). The electronic band and density of states (DOS) calculations reveal that Li_2TlIn crystal is in a metallic structure. Focusing on the elastic properties has shown that this compound is a ductile and mechanically stable material for both ground state and under pressure of 4.53 kbar. In addition, the phonon dispersion curve and the phonon DOS were obtained by density functional perturbation theory. Li_2TlIn has negative frequency values both in the phonon distribution curve and phonon DOS graphs which indicate that Li_2TlIn compound is dynamically unstable in the ground state. However, our results show that, when a pressure of 4.53 kbar is applied, the Li_2TlIn crystal becomes dynamically stable.

Li_2TlIn'in Bazı Fiziksel Özelliklerine Odaklanmak: Bir Temel İlkeler Çalışması

Makale Bilgileri

Geliş: 11.04.2022
Kabul: 25.06.2022
Online Aralık 2022
DOI: 10.53433/yyufbed.1101619

Anahtar Kelimeler
Dinamik özellikler,
Elastik özellikler,
Elektronik özellikler,
Heusler bileşiği,
Li_2TlIn

Öz: Li_2TlIn'in yapısal, elektronik, elastik ve dinamik özellikleri, taban durum (P = 0 kbar) ve 4.53 kbar basınç değeri için, Yoğunluk Fonksiyonel Teorisi (DFT) kullanılarak incelenmiştir. Elektronik bant ve durum yoğunluğu hesaplamaları, Li_2TlIn kristalinin metalik bir yapıda olduğunu ortaya koymaktadır. Elastik özelliklere odaklanmak, bu bileşiğin hem taban durumu hem de 4.53 kbar basınç altında esnek yapıda ve mekanik olarak kararlı bir malzeme olduğunu göstermiştir. Ayrıca yoğunluk fonksiyonel pertürbasyon teorisi ile fonon dağılım eğrisi ve durumların fonon yoğunluğu elde edilmiştir. Li_2TlIn, hem fonon dağılım eğrisinde hem de durumların fonon yoğunluğu grafiklerinde negatif frekans değerlerine sahiptir ve bu, Li_2TlIn bileşiğinin taban durumunda dinamik olarak kararsız olduğunu gösterir. Ancak, sonuçlarımız 4.53 kbar'lık bir basınç uygulandığında Li_2TlIn kristalinin dinamik olarak kararlı hale geldiğini göstermektedir.

1. Introduction

Full-Heusler compounds in the 225 ($Fm\bar{3}m$) space group with Cu_2MnAl crystal structure can be formulated as A_2BC. This structure was discovered by German mining engineer Fritz Heusler (Heusler, 1903). A and B atoms are transition or rare-earth elements, and C atom is the main group element. The atomic coordinates of full-Heusler crystals are (1/4, 1/4, 1/4) and (3/4, 3/4, 3/4) for the A atom and (1/2, 1/2, 1/2) for the B atom and (0, 0, 0) for the C atom (Gilleßen & Dronskowski, 2010). These structures can be semiconductors, metals, topological insulators or semi-metals (Chen & Ren, 2013). There are many studies in the literature that full Heusler compounds are suitable materials for optoelectronic (He et al., 2016), shape memory (Blum et al., 2011), spintronic applications (Bosu et al., 2011; Lei et al., 2011; Galehgirian & Ahmadian, 2015) and thermal barrier coatings (Rasheduzzaman et al., 2021). Therefore, half Heusler (Gupta et al., 2019, 2020 and 2021; Majumder et al., 2020; Majumder & Mitro, 2020) or full Heusler type compounds or alloys have been the subject of researches (Gupta et al., 2022). Ayhan & Kavak Balcı (2019) investigated the properties of the LiX_2Ge (X = Rh, Cu, Pd, Ni) Heusler phase crystals with the first-principles method. Uzunok et al. (2020) examined the physical properties of the $LiGa_2Rh$ crystal with the first-principles method. Rai et al. (2016) calculated and compared the electronic and magnetic properties of X_2YZ and XYZ type Heusler compounds using DFT for different exchange-correlation potentials. Khelfaoui et al. (2018) investigated some physical properties such as magnetic and transport properties of Zr_2PdZ (Z = Al, Ga and In) Heusler compounds with the Generalized Gradient Approximation (GGA). Galdun et al. (2018) have synthesized the intermetallic Co_2FeIn Heusler alloy and suggested that it can be used in spintronic applications. Zipporah et al. (2017) focused on the structural, electronic and magnetic properties of half-Heusler CoVIn and full-Heusler Co_2VIn crystals using DFT and reported that both crystals are semi-metallic materials as a result of their studies. Kamlesh et al. (2021) examined the structural, electronic, optical and thermoelectric properties of XScZ (X = Li, Na, K and Z = C, Si and Ge) half-Heusler compounds and suggested that they may be suitable for photovoltaic devices and thermoelectric applications. Hussain et al. (2018) analyzed the electronic and magnetic properties of Zr_2NiZ (Z = Ga, In, B) crystals using DFT. Rahman et al. (2020) studied on half-Heusler compounds. They reported some physical properties of ScTiX (X = Si, Ge, Pb, In, Sb, Tl,) compounds. Li et al. (2018) determined the electronic and magnetic properties of half-metallic Hf_2VZ (Z = Ga, Tl, In, Si, Ge, Sn and Pb) compounds with first principle computation. In addition, compounds and alloys containing lithium (Li) - thallium (Tl) or lithium (Li) -indium (In) in their structure have been the subject of research. Dogan & Gulebaglan (2021a) analyzed and declared the electronic, elastic and dynamic properties of LiInSi crystal using DFT. Pauly et al. (1968) investigated the structures of Li_2CuTl, Li_2AgTl and Li_2AuTl alloys experimentally. Yahagi et al. (1975) experimentally investigated lattice parameters and structure of LiAlIn and $LiAl_{1-x}In_x$ alloys. Jolayemi et al. (2021) determined the thermoelectric properties of LiAlSi crystal using Boltzmann transport theory and DFT. Dogan & Gulebaglan (2021b) examined and compared the electronic and dynamic properties of Li_2AlIn and Li_2AlGa materials in the Heusler structure. Shah et al. (2018) demonstrated optoelectronic and transport properties of semiconductor LiBZ (B = Al, In, Ga and Z = Si, Ge, Sn) crystals. Siemek et al. (2020) investigated the defect $LiInSe_2$ crystal by optical and positron annihilation spectroscopy. Gavrilova et al. (2021) declared dielectric and pyroelectric properties for lithium-thallium tartrate monohydrate material at temperatures between 2-100 Kelvin. Dogan & Gulebaglan (2022) computed the structural, electronic, elastic, optical and dynamical properties of full Heusler Li_2TlSb and Li_2TlBi crystals.

According to our detailed literature search, Li_2TlIn Heusler compound has not been examined. Its physical properties are not studied, so the physical properties of Li_2TlIn are not known. Only its lattice parameter is given in the "materials Project" web page (Jain et al., 2013). Therefore, in this study we wanted to examine main physical properties of this Heusler compound. The main purpose of this study is to obtain the main physical properties of Li_2TlIn compound, such as structural, electronic, elastic and dynamic properties by using DFT within GGA, before it is synthesized in the laboratory. After calculating the structural and electronic properties the elastic and dynamic properties of Li_2TlIn compound were also computed. All these calculations performed for the ground state (P = 0 kbar) and under a pressure value (P = 4.53 kbar). To date, no extensive researches have been done for the Li_2TlIn compound.

2. Material and Methods

With the DFT, many physical properties of crystal structures can be studied without being in the laboratory environment. With these reviews, both time and cost savings can be achieved. Here, the structural, electronic and dynamic properties of the Li_2TlIn compound, which has not yet been synthesized in the laboratory, were investigated with the Quantum Espresso program (Giannozzi et al., 2009) and the elastic properties were calculated with the Abinit (Gonze et al., 2002) program. Both of these programmes are based on DFT. In order to examine the properties of the Li_2TlIn compound, the GGA proposed by Perdew-Burke-Ernzerhof (Perdew et al., 1997) was used. The energy cutoff value was taken as 80 Ry for both programmes and the charge density cutoff energy value was taken as 320 Ry. The Kohn-Sham (1965) equations were determined using Monkhorst & Pack's (1976) special k-points, which is a set within the Brillouin region. These k-points were used as 12x12x12. Phonon frequencies were analyzed using the linear-response method. Dynamic matrices were created by using Brillouin region 4×4×4 q-points in phonon frequency calculations. Spin-orbit interactions were not considered in the calculations for all the investigated properties. The reason for this is that there is no spin-orbit connection at the pseudopotentials used in the calculations. In order not to make any mistakes in the calculation, care was taken to ensure that the mean error of the energy was less than 1.0×10^{-8} Ry.

3. Results and Discussion

In the beginning, structural properties of the Li_2TlIn (with the space group: $Fm\bar{3}m$ No: 225) were investigated. The structural properties of a material are very important as they provide valuable information about all the physical properties of this material. The coordinates of the four atoms that make up the Li_2TlIn compound are Li(1) (0.25, 0.25, 0.25), Li(2) (0.75, 0.75, 0.75), Tl (0.00, 0.00, 0.00) and In (0.50, 0.50, 0.50). The unit cell form and the bond structure of the Li_2TlIn compound are investigated by Vesta software. The unit cell structure of the Li_2TlIn compound is given in Figure 1. It is noticed that the bond length of Li and In is equal to the bond length of Li and Tl, which is 2.9697 Å.

By using the determined cutoff energy and k-point values, data on the variation of the total energy of the Li_2TlIn compound as a function of volume were created. By fitting these results to the Birch-Murnaghan equation (Birch, 1947), the lattice constant, Bulk modulus (describes the resistance of a material to the compressibility) and the derivative of the Bulk modulus with respect to the pressure (related to the thermoelastic properties of the material) were calculated for the ground state. The Birch-Murnaghan equation is a temperature-independent isothermal equation and is one of the equations frequently used to determine the isothermal behavior of solids that are under pressure.

$$E(V) = E_0 + \frac{9V_0B_0}{16}\left\{\left[\left(\frac{V_0}{V}\right)^{2/3} - 1\right]^3 B_0^{'} + \left[\left(\frac{V_0}{V}\right)^{2/3} - 1\right]^2 \left[6 - 4\left(\frac{V_0}{V}\right)^{2/3}\right]\right\} \quad (1)$$

Here, E_0, V_0, B_0 and B_0' are the total energy, volume, Bulk modulus and the first derivative of the Bulk modulus relative to pressure, respectively (Table 1). In this study, the Bulk modulus was also calculated in the elastic properties part (Table 3). The two Bulk modulus results within this study are in good agreement with each other. The lattice constant value for the Li_2TlIn compound calculated in this study is $a_{Li2TlIn}$ = 6.77 Å which is in good agreement with the previous result (Jain et al., 2013). The lattice parameter is directly proportional to the volume of that material. If the volume is large, the lattice parameter is also large. However, the Bulk modulus is inversely proportional to the volume or lattice parameter. If the lattice parameter is large the Bulk modulus becomes small in value. In other words, for a bigger material, the Bulk modulus is small, which means that the resistance of a material to compressibility is small for materials having long lattice parameters. Additionally, the derivative of the Bulk modulus is inversely proportional to the Bulk modulus itself. The derivative of the Bulk modulus is small when the Bulk modulus is high. The values of structural properties are compatible with our previous studies (Dogan & Gulebaglan, 2021a and 2022).

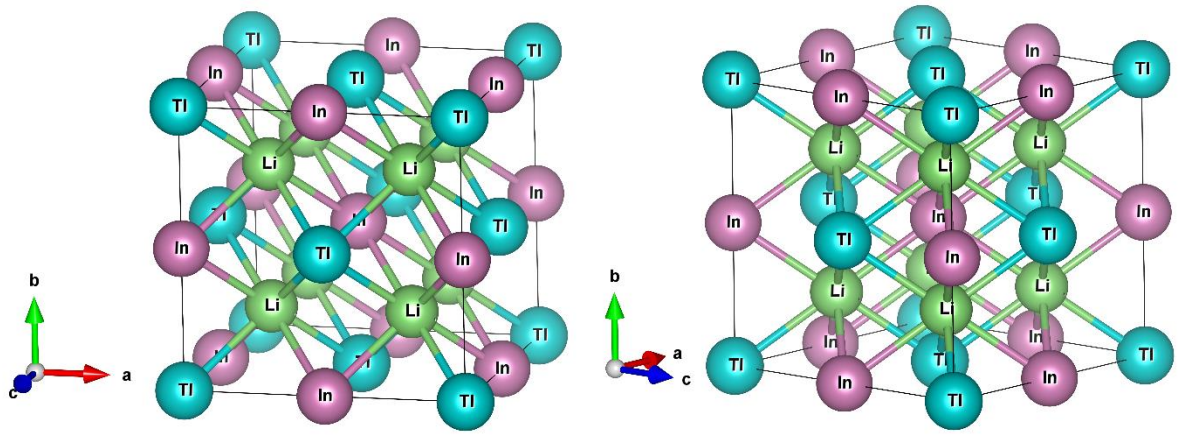

Figure 1. Optimized crystal structure of Li_2TlIn.

Table 1. Structural parameters for the Li_2TlIn Heusler compound

	a (Å)	B (GPa)	B_0'
Li_2TlIn (Present Work)	6.77	27.1	7.65
Ref. (Jain et al., 2013)	6.96		

Then, the electronic band structure was investigated for the Li_2TlIn compound to examine its electronic properties, and the energy band diagram for the Li_2TlIn compound is given in Figure 2. The electronic band diagram is drawn along the high symmetry points of Γ→X→W→L→Γ→K→W→U in the first Brillouin region. In the band structure graph for Li_2TlIn, the Fermi level is set to an energy level of 0 eV. As can be seen in Figure 2, the core electron states are seen at energies around - 10 eV. The minimum energy value of the conduction band is below the Fermi level. Also, the maximum energy value of the valance band is over the Fermi level, which indicates that Li_2TlIn Heusler alloys are metallic in structure. Also for semimetals, there is an overlapping of the valance and the conduction bands, however, this should be a slight overlapping. Also, we can decide whether a material is a metal or semimetal by looking at the DOS graph. For a semimetal, the DOS value at the Fermi level must be very small but for metal, it must be large. In Figure 3, it is clearly seen that the DOS value at the Fermi level is very large, so Li_2TlIn is of metallic nature, which is also compatible with the literature (e.g. Gupta et al., 2020 and 2022). The total DOS and the partial DOS (PDOS) of the Li_2TlIn crystal were investigated with the Abinit program using GGA. The Fermi energy level is also shown in the DOS and the PDOS graphs with a vertical red line. The DOS graph is compatible with the electronic band diagram. Also from the DOS graph, it is seen that this compound has no bandgap. In order to identify the contributions of the Li, Tl and In atoms to the electronic band structure individually, the PDOS graphs of those atoms were also plotted as given in Figure 3. The heavy contribution to the conduction bands comes mainly from the Li (1) and Li (2) atoms with the p (dominantly), s and d states. Both Li atoms slightly contribute to the valance band with p and s states. The contribution of Tl and In atoms look like each other. Both have a peak value with s state in the valance band. These atoms have also contributions to both valance and conduction bands with s and p states.

The dynamic properties of Li_2TlIn compound were also studied in the ground state and under the pressure value of 4.53 kbar. The pressure of 4.53 kbar is necessary to make the compound dynamically stable because in the ground state Li_2TlIn compound is dynamically unstable. We investigated the impact of this amount of pressure on the electronic structure of the Li_2TlIn compound. We found that the pressure of 4.53 kbar did not have an effect on the electronic properties of the Li_2TlIn compound. The electronic band diagram, DOS, and PDOS graphs are almost the same for both; the ground state and 4.53 kbar pressure. Therefore, it is noticed that this small amount of pressure does not affect the electronic properties of the Li_2TlIn compound.

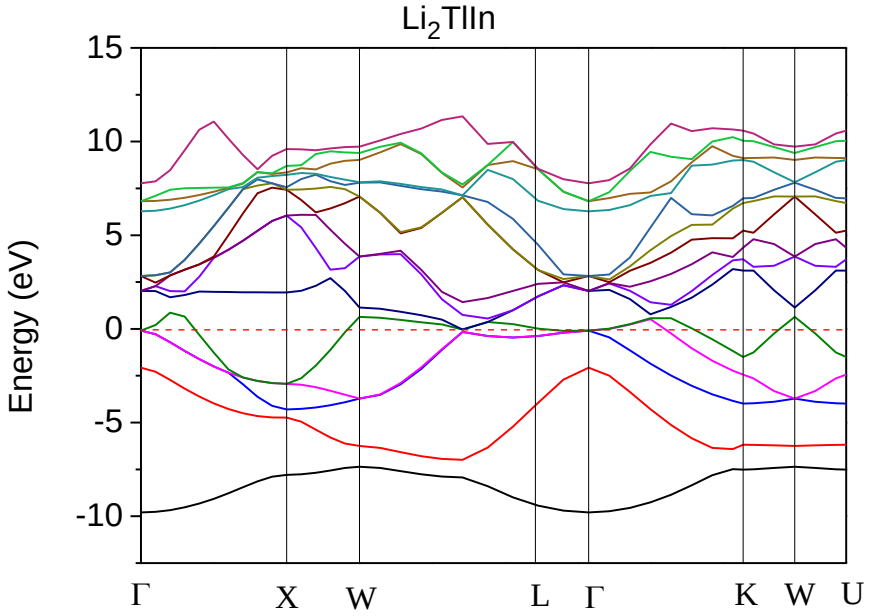

Figure 2. Calculated electronic band diagram of Li_2TlIn compound. The Fermi energy level is matched to 0 eV and given with horizontal line.

Afterwards, we focused on the elastic properties of Li_2TlIn. First, the elastic constants (C_{ijkl}) were calculated. Elastic constants are four rank tensors and they have 81 components. Because of some symmetry properties of elastic constants ($C_{ijkl} = C_{jikl}$ and $C_{ijkl} = C_{ijlk}$) and by using a matrix notation the number of components decreases to 36 (Nye, 1985). By using matrix notation, elastic constants can be shown with two indices such as C_{mn}, but it is not a "two rank tensor". However, since $C_{mn} = C_{nm}$, the number of independent components decreases to 21. According to the crystal structures, the number of elastic constants changes. For cubic structures, there are 3 independent components of elastic constants, namely, C_{11}, C_{12} and C_{44}. C_{11} gives information about the stiffness against primary strains, C_{12} is related to the transverse expansion and C_{44} shows the amount of opposition to the shear deformation. In this study, the elastic constants in the ground state and under 4.53 kbar pressure values are calculated and compared with each other (Table 2). When pressure increases, the elastic values increase as seen from Table 2. By using elastic constants the elastic properties, mechanical stability and ductile-fragile property of a compound can be revealed. Here the Bulk, Shear and Young modulus, Poisson ratio, Flexibility (Pugh's ratio) coefficient and Debye temperature of Li_2TlIn for ground state (P = 0 kbar) and under 4.53 kbar pressure value were calculated and all of them are given in Table 3. Bulk modulus shows the physical phenomena of compressibility. If the Bulk modulus value is high, its compressibility property gets low. Shear modulus is related to the resistance of that material to the deformation of the shape. It also gives information about the hardness of the material. The shear modulus and stiffness constant C_{44} are related to the hardness and the resistance to shear deformation (Gilman, 1997). Our calculations indicate that shear modulus and C_{44} are not very high, meaning that the Li_2TlIn is not very hard material. However, increasing the pressure to a small amount (i. e. 4.53 kbar) makes Li_2TlIn harder since shear modulus and C_{44} increases with the pressure.

Young's modulus is equal to the ratio of the tensile stress to the tensile strain which shows the stiffness of the compound. The Poisson ratio is very useful to better understand the ductile or brittle properties of a material. If the Poisson ratio is smaller than 0.26, the material is said to be brittle. However, if the ratio is higher than 0.26, the material is said to be ductile. Also, we calculated the Flexibility coefficient which is also known as Pugh's ratio. This flexibility coefficient is also important to understand again the ductile or brittle structure of a material. If the calculated value is bigger than 1.75 that material is ductile otherwise that material is brittle in structure. The Debye temperature is directly related to the energies of the high-frequency modes. In this study, we calculated the Debye temperature as 72.72 K for the ground state and as 80.91 K under 4.53 kbar pressure. The energies of

the high-frequency modes above the Debye temperature become equal to k_BT and under the Debye temperature, they would be frozen (Turney et al., 2009).

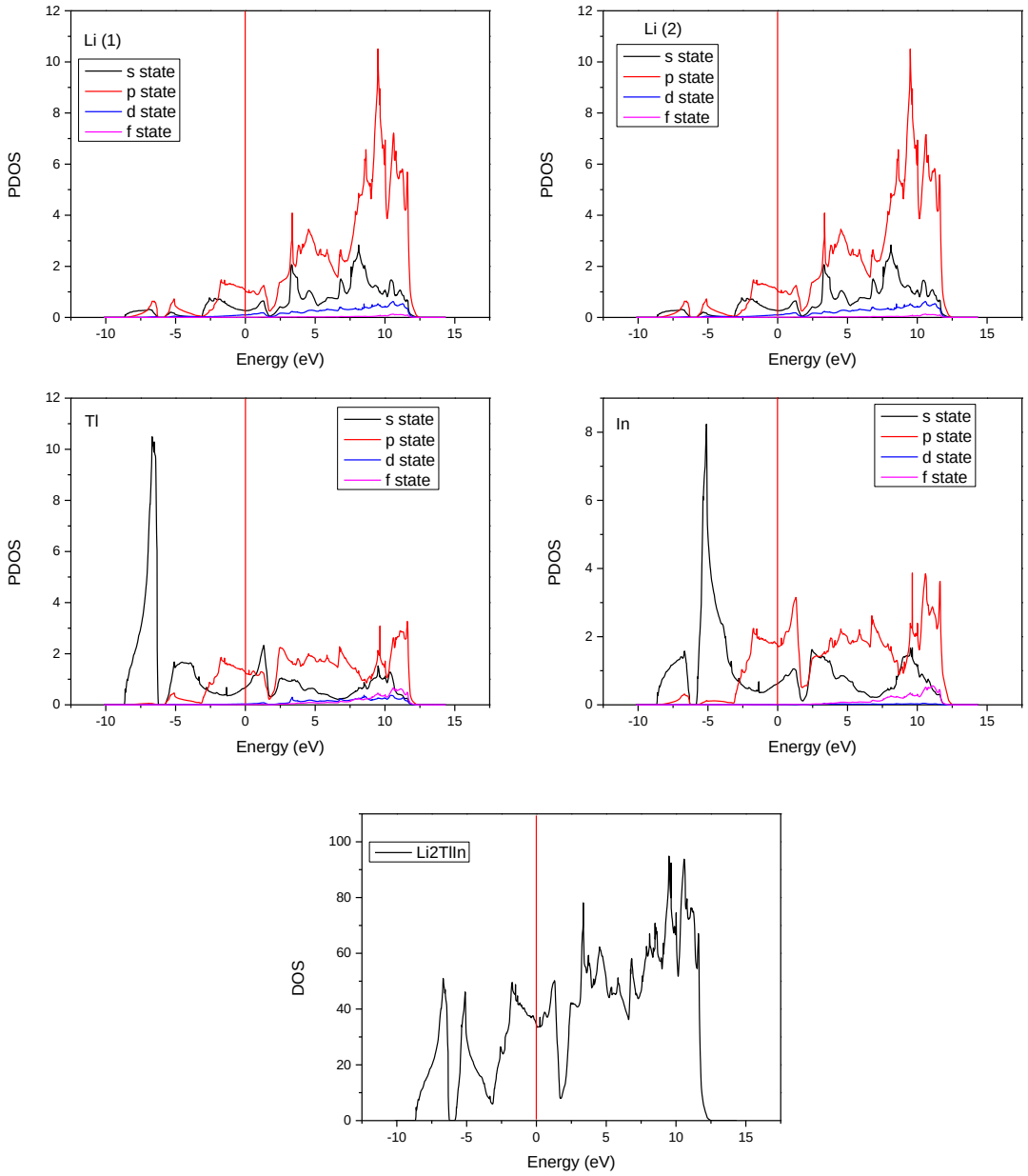

Figure 3. The total DOS and partial density of states (PDOS) graphs of the Li_2TlIn compound. The Fermi level is shown with a vertical red line at 0 eV.

There are approaches used to calculate the Bulk and Shear moduli, such as Voight, Reuss and Hill. For the Voight approach, elastic stiffness constants (C_{ij}) are used, meanwhile for the Reuss approach the elastic compliance constants (S_{ij}) are used. The relation between the elastic stiffness constant and the compliance constant can be given as, $1 = C_{ij}.S_{ij.}$ The Hill approach is the average value of Voight and Reuss's approaches. The values of Bulk modulus are equal to each other within the three approaches and also with the value that is obtained during the investigation of the structural properties of the Li_2TlIn compound. The Shear modulus values are also very akin to each other within three approaches. As seen in Table 3, when the pressure increases, the values of all elastic properties increase.

Table 2. The elastic constants of Li_2TlIn compound

Pressure (kbar)	C_{11} (GPa) $(= C_{22} = C_{33})$	C_{12} (GPa) $(= C_{13} = C_{21} = C_{23} = C_{31} = C_{32})$	C_{44} (GPa) $(= C_{55} = C_{66})$
0	43.34	27.18	29.16
4.53	53.55	32.62	35.17

Table 3. The Bulk, Shear, Young modulus, Poisson ratio, Flexibility coefficient and Debye temperature of Li_2TlIn compound

Elastic Property of Li2TlIn	Symbol (unit)	P = 0 kbar	P = 4.53 kbar
Voight Bulk Modulus	B_V (GPa)	32.57	39.60
Reuss Bulk Modulus	B_R (GPa)	32.57	39.60
Hill Bulk Modulus	B_{VRH} (GPa)	32.57	39.60
Voight Shear Modulus	G_V (GPa)	20.73	25.29
Reuss Shear Modulus	G_R (GPa)	14.27	18.09
Hill Shear Modulus	G_{VRH} (GPa)	17.50	21.69
Young Modulus	E (GPa)	44.52	55.02
Poisson Ratio	v (-)	0.27	0.27
Flexibility Coefficient	$K = B_{VRH}/G_{VRH}$ (-)	1.85	1.84
Debye Temperature (K)	Θ_D	72.72	80.91

If a material satisfies the Born criterias (Mouhat & Coudert, 2014), then that material is mechanically stable. These criterias are given in the following:

$$\begin{aligned} &\text{i) } C_{11} + 2C_{12} > 0, \\ &\text{ii) } C_{44} > 0, \\ &\text{iii) } C_{11} - C_{12} > 0\ , \\ &\text{iv) } C_{11} > 0 \\ &\text{v) } C_{12} < B < C_{11} \end{aligned} \tag{2}$$

where B is the Bulk modulus. Since the elastic constants satisfy these criteria, Li_2TlIn compound is mechanically stable for ground state and under 4.53 kbar pressure value.

The calculated Poisson ratio and flexibility coefficient show that Li_2TlIn is ductile in the ground state and under 4.53 kbar pressure. Because the values above 1.75 for flexibility coefficient and 0.26 for Poisson ratio show that material is ductile. As a result, it can be concluded as Li_2TlIn is a ductile (elastic) in structure, and it is not very hard.

The Debye temperature also gives information about the thermal conductivity of a compound (Toher et al., 2014). If the thermal conductivity property is high, the Debye temperature of that compound is also high. The thermal conductivity of the Li_2TlIn increases by increasing the pressure.

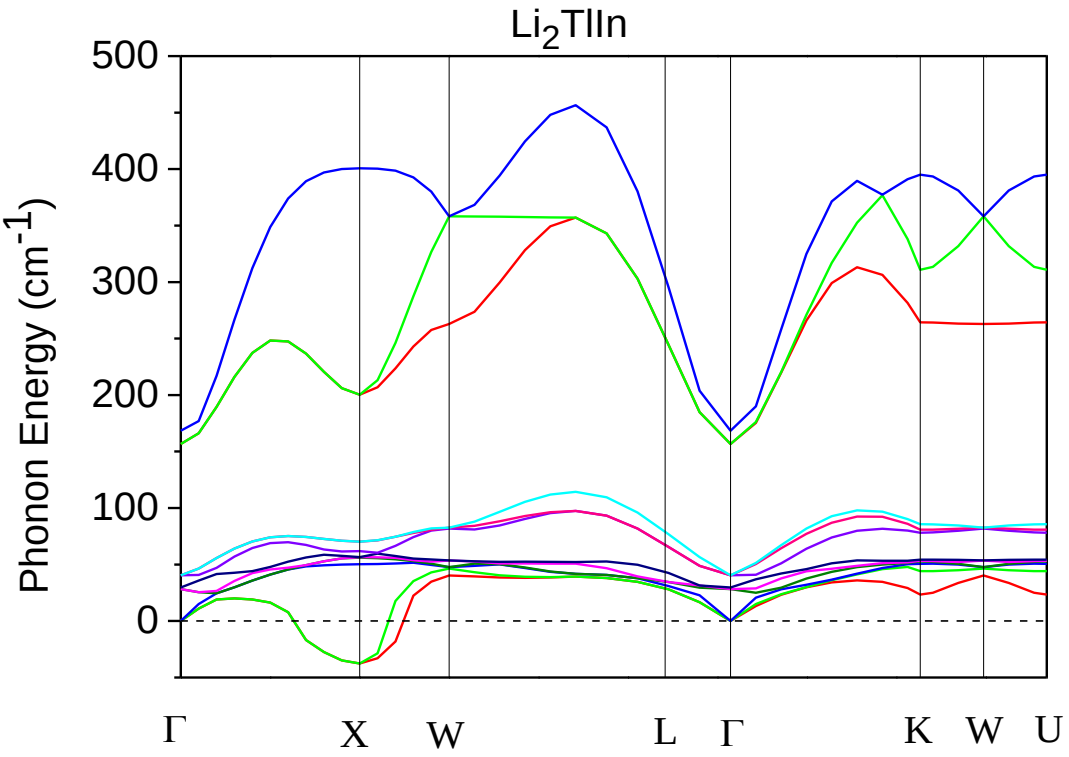

Figure 4. Phonon dispersion graph of the Li_2TlIn compound in the ground state.

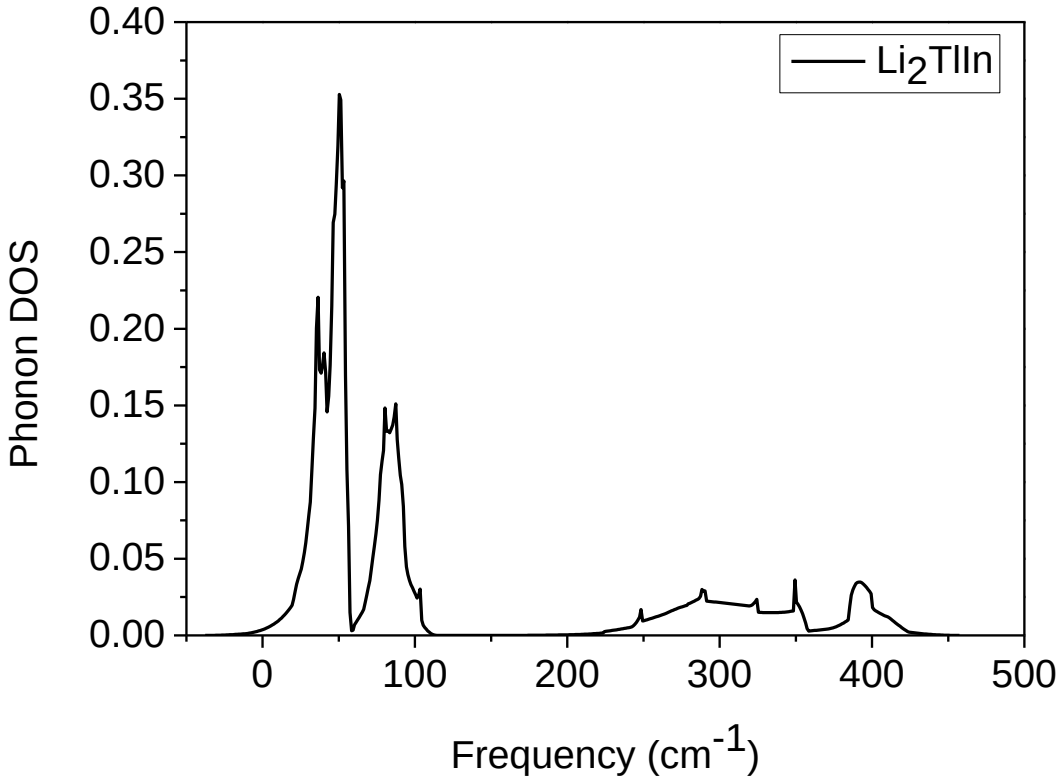

Figure 5. The phonon DOS graph of the Li_2TlIn in the ground state.

Afterwards, we concentrated on the dynamical properties of the Li_2TlIn compound. The phonon dispersion curve and phonon DOS graphs were obtained, which are given in Figures 4 and 5, respectively. Since in its unit cell, Li_2TlIn has 4 atoms, 12 phonon modes occur. The 3 of them are

acoustic modes, and the 9 of them are optic modes. The acoustic modes have the lowest photon frequency. Two of them are transverse acoustic (TA) and one of them is longitudinal acoustic (LA) mode. The transverse modes have smaller frequencies than longitudinal modes. Similarly, 3 of the optic modes are longitudinal optic (LO) modes, and 6 of them are transverse optic (TO) modes.

The phonon dispersion curve of the Li_2TlIn compound in the ground state was obtained by plotting the phonon energies with respect to the Γ→X→W→L→Γ→K→W→U high symmetry points (Figure 4). The phonon DOS graph was also obtained in the ground state. Both of these graphs have shown that the Li_2TlIn compound has negative frequency values, indicating the Li_2TlIn compound is dynamically unstable. The net force on the atoms that compose Li_2TlIn is not equal to zero, which means, this compound is not decisive in the ground state (P = 0 kbar). If one exerts a force on a compound, that compound may become stable. By increasing the value of the pressure the phonon frequencies increase, and negative phonon frequencies become positive. We wanted to find that pressure value, which makes this compound dynamically stable when exerted on it. We found that when 4.53 kbar pressure is exerted on Li_2TlIn, it becomes dynamically stable because the phonon dispersion curve (Figure 6) and the phonon DOS graphs (Figure 7) have no negative frequency values under P = 4.53 kbar.

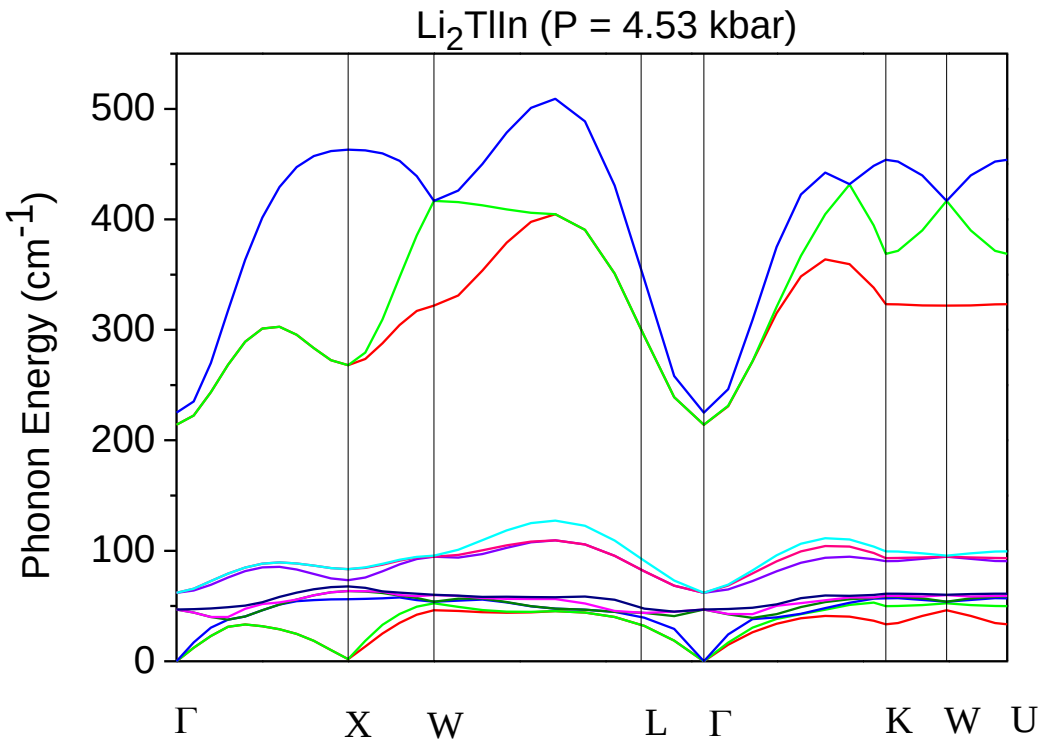

Figure 6. Phonon dispersion curves of the Li_2TlIn compound under thr pressure of 4.53 kbar.

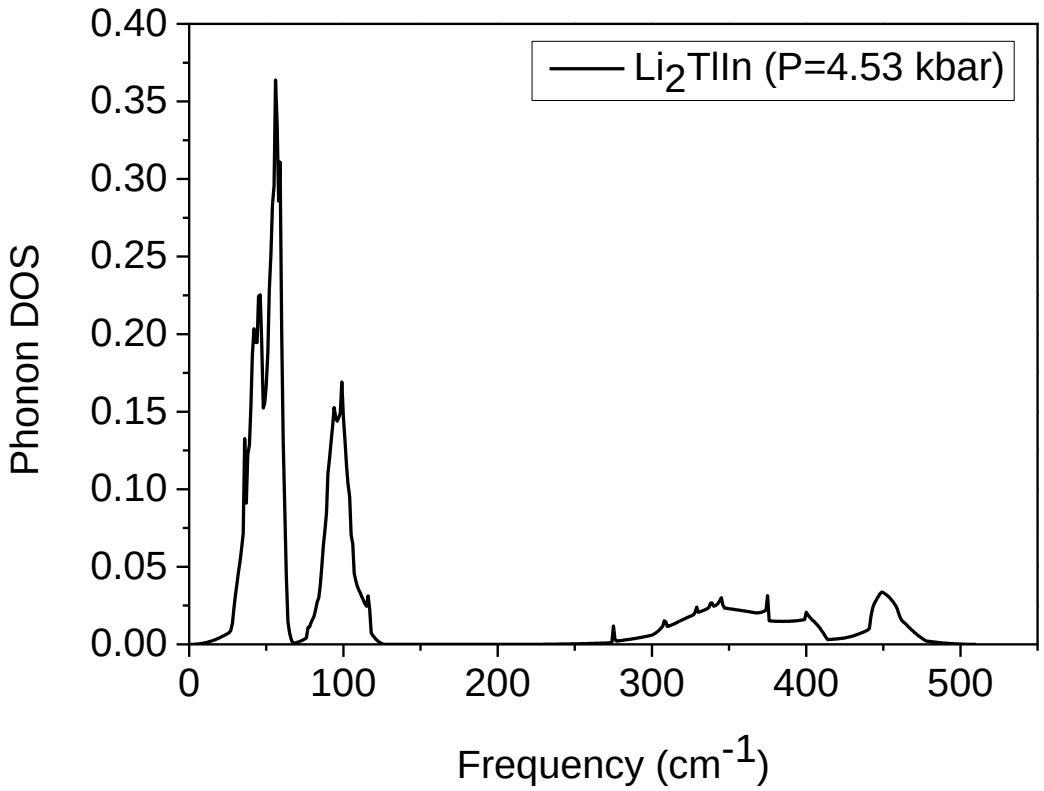

Figure 7. Phonon DOS of the Li_2TlIn compound for the pressure of 4.53 kbar.

When one examines Figure 6 (and Figure 7), it is seen that there are almost three phonon bands. The first one with the smallest frequency is composed of 3 acoustic (2 TA and 1 LA) and 3 optic (2 TO and 1LO) modes. This is the band that has the biggest contribution to the phonon DOS (Figure 7). The second band occurred around 100 cm^{-1} frequency value and was composed of three optic modes (2 TO and 1 LO). The third band with the highest frequency values has a very wide frequency width, nearly 200 cm^{-1}, composed of 3 optic modes.

Phonon dispersion graphs (Figures 4 and 6) show that there is a degeneracy between the TA modes and also there are degeneracies on consecutive TO modes, which clearly explains the symmetry property of the Li_2TlIn compound is very high.

The other effect of the increasing pressure is increasing the frequency of the longitudinal optic mode with high frequency. Because when pressure is exerted on a compound, its lattice parameters become smaller. A smaller lattice parameter gives a force constant a higher value that causes to increase in phonon frequency. When one examines Figures 4-7, it is clear that when the pressure is applied the maximum value of the phonon frequency is increased by 50 cm^{-1}.

A factor group analysis was also performed in order to obtain the irreducible representation of Γ for the Li_2TlIn compound by using the Bilbao crystallographic server (Aroyo et al., 2006). The space group of Li_2TlIn is $Fm\bar{3}m$ (No: 225) and the point group is O_h ($m\bar{3}m$). The irreducible representation of Γ is obtained as follows:

$$\Gamma = \Gamma_{acoustic} + \Gamma_{optic} \tag{3}$$

$$\Gamma_{acoustic} = T_{1u} \tag{4}$$

$$\Gamma_{optic} = T_{2g} + 2T_{1u} \tag{5}$$

In the elastic properties part, the Debye temperature was argued and it was mentioned that Debye temperature is related with the thermal conductivity of a material. Transverse acoustic modes are directly related with the thermal conductivity of a compound. If these TA modes are not scattered,

then that material has a high thermal property (Neilsen et al., 2013). If transverse optic (TO) modes and TA modes coincide together, TA modes are scattered. Figure 6 shows that TO modes do not coincide with TA modes. But with a detailed examination, TA and TO modes take the same frequency values at W high symmetry point. This means Li_2TlIn has a thermal property but it is not very high. Also calculated Debye temperature value satisfies this result.

4. Conclusion

In this study, some physical properties of the Li_2TlIn compound were investigated in the ground state and under the pressure value of P = 4.53 kbar by using DFT within GGA. The calculated lattice parameter of Li_2TlIn is in a good agreement with the previous study. Also, the Bulk modulus and the derivative of the Bulk modulus with respect to the pressure were investigated. The electronic band diagram, the total DOS and partial DOS are investigated in the ground state and under 4.53 kbar pressure. Since the electronic properties were not affected by this amount of pressure, here we only gave the plots of the ground state. The electronic band diagram and the DOS graphs show that Li_2TlIn is a metal. By calculating the elastic properties, it is noticed that the Li_2TlIn compound is not fragile, it is ductile material and it is mechanically stable both in the ground state and under pressure. Finally, the dynamic properties were investigated by plotting the phonon dispersion and phonon DOS graphs. For the ground state (P = 0 kbar) Li_2TlIn is dynamically unstable, however, we showed that under 4.53 kbar pressure Li_2TlIn becomes dynamically stable. The phonon dispersion graph and calculated Debye temperature value revealed that Li_2TlIn has a low thermal conductivity property. Only the lattice parameter value could be compared with the literature. The rest of the results are performed for the first time in the literature. Therefore, it is believed that this study will be very useful for researchers in future studies.

References

Aroyo, M. I., Perez-Mato, J. M., Capillas, C., Kroumova, E., Ivantchev, S., Madariaga, G., & Kirov, A. (2006). Bilbao crystallographic server: I. Databases and crystallographic computing programs. *Zeitschrift für Kristallographie,* 221(1), 15-27. doi: 10.1524/zkri.2006.221.1.15

Ayhan, S., & Kavak Balcı, G. (2019). Ab-initio calculations structural electronic and elastic properties of LiX_2Ge (X = Rh, Cu, Ni, Pd) Heusler compounds. *Materials Research Express,* 6, 0865e9. doi: 10.1088/2053-1591/ab250c

Birch, F. (1947). Finite Elastic Strain of Cubic Crystals. *Physical Review*, 71, 809-824. doi: 10.1103/PhysRev.71.809

Blum, C. G. F., Ouardi, S., Fecher, G. H., Balke, B., Kozina, X., Stryganyuk, G., Ueda, S., Kobayashi, K., Fesler, C., Wurmehl, S., & Büchner, B. (2011). Exploring the details of the martensite-austenite phase transition of the shape memory Heusler compound Mn_2NiGa by hard x-ray photoelectron spectroscopy, magnetic and transport measurements. *Applied Physics Letters*, 98, 252501. doi: 10.1063/1.3600663

Bosu, S., Sakuraba, Y., Uchida, K., Saito, K., Ota, T., Saitoh, E., & Takanashi, K. (2011). Spin seeback effect in thin films of the Heusler compound Co_2MnSi. *Physical Review B,* 83, 224401. doi: 10.1103/PhysRevB.83.224401

Chen, S., & Ren, Z. (2013). Recent progress of half-Heusler for moderate temperature thermoelectric applications. *Materials Today,* 16(10), 387-395. doi: 10.1016/j.mattod.2013.09.015

Dogan, E. K., & Gulebaglan, S. E. (2021a). Some properties of LiInSi half-Heusler alloy via density functional theory. *Bulletin of Materials Science,* 44, 208. doi: 10.1007/s12034-021-02499-y

Dogan, E. K., & Gulebaglan, S. E. (2021b). Lattice dynamics and electronic properties of heusler alloys Li_2AlX (X = Ga, In): a comparison study. *Chinese Journal of Chemical Physics,* 34, 173-178. doi: 10.1063/1674-0068/cjcp2008151

Dogan, E. K., & Gulebaglan, S. E. (2022). A computational estimation on structural, electronic, elastic, optic and dynamic properties of Li_2TlA (A = Sb and Bi): First-principles calculations. *Materials Science in Semiconductor Processing,* 138, 106302. doi: 10.1016/j.mssp.2021.106302

Galdun, L., Vega, V., Vargova, Z., Barriga-Castro, E. D., Luna, C., Varga, R., & Prida, V. M. (2018). Intermetalic Co_2FeIn Heusler Alloy Nanowires for spintronic Applications. *ACS Applied Nano Materials*, 1(12), 7066-7074. doi: 10.1021/acsanm.8b01836

Galehgirian, S., & Ahmadian F. (2015). First principles study on half-metalilic properties of Heusler compounds Ti_2VZ (Z = Al, Ga and In). *Solid States Communications*, 202, 52-57. doi: 10.1016/j.ssc.2014.10.017

Gavrilova, N. D., Malyshkina, I. A., & Novik, O. D. (2021). Hydrogen band as a trigger of ferroelectric-like phase transition in lithium-thallium tartrate monohydrate. *Ferroelectrics*, 582, 1-11. doi: 10.1080/00150193.2021.1951029

Giannozzi, S., Bonini, N., Calandra, M., Car, R., Cavazzoni, C., Ceresoli, D., Chiarotti, G. L., Cococcioni, M., Dabo, I., Corso, A. D., de Gironcoli, S., Fabris, S., Fratesi, G., Gebauer, R., Gerstmann, U., Gougoussis, C., Kokalj, A., Lazzeri, M., Samos, L. M., Marzari, N., Mauri, F., Mazzarello, R., Paolini, S., Pasquarello, A., Paulatto, L., Sbraccia, C., Scandolo, S., Sclauzero, G., Seitsonen, A. P., Smogunov, A., Umari, P., & Wentzcovitch, R. M. (2009). QUANTUM ESPRESSO: a modular and open-source software project for quantum simulations of materials. *Journal of Physics: Condensed Matter*, 21, 395502. doi: 10.1088/0953-8984/21/39/395502

Gilleßen, M., & Dronskowski, R. (2010). A combinatorial study of inverse Heusler alloys by first-principles computational methods. *Journal of Computational Chemistry*, 31, 612-619. doi: 10.1002/jcc.21358.

Gilman, J. J. (1997). Chemical and physical "hardness". *Materials Research Innovations*, 1, 71–76.

Gonze, X., Beuken, J. M., Caracas, R., Detraux, F., Fuch, M., Rignanese, G. M., Sindic, L., Verstrate, M., Zerah, G., Jollet, F., Torrent, M., Roy, A., Mikami, M., Ghosez, P., Raty, J. Y., & Allan, D. C. (2002). First-principles computation of material properties: the ABINIT software Project. *Computational Materials Science*, 25, 478-492. doi: 10.1016/S0927-0256(02)00325-7

Gupta, Y., Sinha, M. M., & Verma, S. S. (2019, June). *Structural and lattice dynamical study of half Heusler alloys RuMnX (X = P, As).* Proceedings of the International Conference on Advanced Materials: ICAM, India.

Gupta, Y., Sinha, M. M., & Verma, S. S. (2020). Theoretical study of structural, electronic and lattice dynamical properties of novel AlNiP half-Heusler alloy. *Philosophical Magazine*, 100, 2785. doi: 10.1080/14786435.2020.1792570

Gupta, Y., Sinha, M. M., & Verma, S. S. (2021). Investigations of mechanical and thermoelectric properties of 'AlNiP' novel half-Heusler alloy. *Materials Chemistry and Physics*, 265, 124518. doi: 10.1016/j.matchemphys.2021.124518.

Gupta, Y., Sinha, M. M., & Verma, S. S. (2022). Effect of spin-polarization on structural, electronic, and lattice dynamical properties of 'MnY2Ga' full Heusler alloy. *Physica B*, 624, 413425. doi: 10.1016/j.physb.2021.413425

He, J., Amsler, M., Xia, Y., Naghavi, S. S., Hegde, V. I., Hao, S., Goadecter, S., Ozolins, V., & Wolverton, C. (2016). Ultralow Thermal Conductivity in Full Heusler Semiconductors. *Physical Review Letters*, 117, 046602. doi: 10.1103/PhysRevLett.117.046602

Heusler, F. (1903). Über magnetische manganlegierungen. *Verhandlungen der DPG*, 5, 219-224.

Hussain, M. K., Hassan, O. T., & Algubili, A. M. (2018). Investigation of the electronic and magnetic structures of Zr_2NiZ (Z = Ga, In, B) Heusler compounds; first principles study. *Journal of Electronic Materials*, 47, 6221. doi: 10.1007/s11664-018-6512-2

Jain, A., Ong, S. P., Hautier, G., Chen, W., Richards, W., Davidson, D. S., Cholia, S., Gunter, D., Skinner, D., Ceder, G., & Persson, K. (2013). Commentary: The Materials Project: A materials genome approach to accelerating materials innovation. *APL Materials*, 1, 011002. doi: 10.1063/1.4812323

Jolayemi, O. R., Adetunji, B. I., Ozafile, O. E., & Adebayo, G. A. (2021). Investigation of the thermoelectric properties of Lithium-Aluminium-Silicide (LiAlSi) compound from first principles calculations. *Computational Condensed Matter*, 27, e00551. doi: 10.1016/j.cocom.2021.e00551

Kamlesh, P. K., Gautam, R., Kumari, S., & Verma, A. S. (2021). Investigation of inherent properties of XScZ (X = Li, Na, K; Z = C, Si, Ge) half Heusler compounds: Appropriate for photovoltaic

and thermoelectric applications. *Physica B: Condensed Matter,* 615, 412536. doi: 10.1016/j.physb.2020.412536

Khelfaoui, F., Boudali, A., Bentayeb, A., El Hachemi Omari, L., & Abderrahmane, Y. S. (2018). Investigation of structural, elastic, electronic, magnetic and transport properties of the Heusler compounds Zr_2PdZ (Z = Al, Ga and In): FP-LAPW method. *Acta Physica Polanica A,* 133, 157-163. doi:10.12693/APhysPolA.133.157

Kohn, W., & Sham, L. J. (1965). Self-consistent equations including exchange and correlation effects. *Physical Review*, 140, 1133-1138. doi: 10.1103/PhysRev.140.A1133

Lei, F., Tang, C., Wang, S., & He, W. (2011). Half metallic full Heusler compound Ti_2NiAl: A first principles study. *Journal of Alloys and Compounds,* 509, 5187-5189. doi:10.1016/j.jallcom.2011.02.002

Li, Y., Liu, G. D., Wang, X. T., Zhao, W. Q., Liu, E. K., Xi, X. K., Wang, W. H., Wu, G. H., & Dai, X. F. (2018). Electronic structures magnetic properties and half-matallicity of Heusler compounds Hf_2VZ (Z = Ga, In, Tl, Si, Ge, Sn and Pb): First principles calculations. *Journal of Superconductivity and Novel Magnetism,* 31, 3063-3074. doi: 10.1007/s10948-017-4544-0

Majumder, R., & Mitro, S. K. (2020). Justification of crystal stability and origin of transport properties in ternary half-Heusler ScPtBi. *RSC Advances,* 10, 37482. doi: 10.1039/d0ra06826h

Majumder, R., Mitro, S. K., & Bairagi B. (2020). Influence of metalloid antimony on the physical properties of palladium-based half-Heusler compared to the metallic bismuth: A first-principle study. *Journal of Alloys and Compounds,* 836,155395. doi: 10.1016/j.jallcom.2020.155395

Monkhorst, H., & Pack, J. D. (1976). Special points for Brillouin-zone integrations. *Physical Review B,* 13, 5188-5192. doi: 10.1103/PhysRevB.13.5188

Mouhat, F., & Coudert, F. X. (2014). Necessary and sufficient elastic stability conditions in various crystal systems. *Physical Review B,* 90, 224104. doi: 10.1103/PhysRevB.90.224104

Nielsen, M. D., Ozolins, V., & Heremans, J. P. (2013). Lone pair electrons minimize lattice thermal conductivity. *Energy & Environmental Science,* 6, 570-578. doi:10.1039/c2ee23391f

Nye, J. F. (1985). *Physical Properties of Crystals: Their Representation by Tensors and Matrices.* New York: Oxford University Press.

Pauly, H., Weiss, A., & Witte, H. (1968). The crystal structure of the ternary intermetallice phases Li2 EX (E = Cu,Ag,Au; X = Al,Ga,In,Tl1,S1,Ge, Sn,Pb,Sb,Bi). *Zeitschrift für Metallkunde,* 59, 47. doi: 10.1515/ijmr-1968-590106

Perdew, J. P., Burke, K., & Ernzerhof, M. (1997). Generalized gradient approximation made simple. *Physical Review Letters*, 78, 1396. doi: 10.1103/PhysRevLett.77.3865

Rahman, N., Husain, M., Yang, J., Murtaza, G., Sjjad, M., Habib, A., Zulfiqar, A. K., Ul Haq, M., Rauf, A., Nisar, M., & Khan, M. Y. (2020). First principles study of structural electronic elastic and magnetic properties of Half- Heusler Compounds ScTiX (X = Si, Ge, Pb, In, Sb and Tl). *Journal of Superconductivity and Novel Magnetism,* 33, 3915. doi: 10.1007/s10948-020-05652-6

Rai, D. P. R., Sandeep, Shankar, A., Sakhya, A. P., Sinha, T. P., Khenata, R., Ghimire, M. P., & Thapa, R. K. (2016). Electronic and magnetic properties of X_2YZ and XYZ Heusler compounds a comparative study of density functional teory with different exchange correlation potentials. *Materials Research Express,* 3, 075022. doi: 10.1088/2053-1591/3/7/075022

Rasheduzzaman, Md., Hossain, K. M., Mitro, S. K., Hadi, M. A., Modak, J. K., & Hasan, Md. Z. (2021). Structural, mechanical, thermal, and optical properties of inverse-Heusler alloys Cr2CoZ (Z=Al, In): A first-principles investigation. *Physics Letters A,* 385, 126967. doi: 10.1016/j.physleta.2020.126967

Shah, S. H., Khan, S. H., Laref, A., & Murtaza, G. (2018). Optoelectronic and transport properties of LiBZ (B = Al, In, Ga and Z = Si, Ge, Sn) semiconductors. *Journal of Solid State Chemistry,* 258, 800-808. doi: 10.1016/j.jssc.2017.12.014

Siemek, K., Yelisseyev, A. P., Horoek, P., Lobanov, S. I., Goloshumova, A. A., Belushkin, A. V., & Isaenko, L. I. (2020). Optical and positron annihilation studies of structural defects in $LiInSe_2$ single crystals. *Optical Materials,* 109, 110262. doi: 10.1016/j.optmat.2020.110262

Toher, C., Plata, J. J., Levy, O., de Jong, M., Asta, M., Nardelli, M. B., & Curtarolo, S. (2014). High-throughput computational screening of thermal conductivity, Debye temperature, and

Gr¨uneisen parameter using a quasiharmonic Debye model. *Physical Review*, 90, 174107. doi: 10.1103/physrevb.90.174107

Turney, J. E., McGaughey, A. J. H., & Amon, C. H. (2009). Assessing the applicability of quantum corrections to classical thermal conductivity predictions. *Physical Review B*, 79, 224305. doi: 10.1103/physrevb.79.224305

Uzunok, H. Y., Karaca, E., Bağcı, S., & Tütüncü, H. M. (2020). Physical properties and superconductivity of Heusler compound $LiGa_2Rh$: A first principles calculation. *Solid State Communications*, 311, 113859. doi: 10.1016/j.ssc.2020.113859

Yahagi, M., Kuriyama, K., & Iwamura, K. (1975). X-ray study of LiAl1-xInx and Li2AlIn. *Japanese Journal of Applied Physics*, 4, 405.

Zipporah, M., Rohit, P., Robinson, M., Julius, M., Ralph, S., & Arti, K. (2017). First principles investigation of structural electronic and magnetic properties of Co_2VIn and CoVIn Heusler compounds. *AIP Advances*, 7, 055705. doi: 10.1063/1.4973763